Learning correspondences of cardiac motion from images using biomechanics-informed modeling

Xiaoran Zhang[1], Chenyu You[2], Shawn Ahn[1], Juntang Zhuang[1], Lawrence Staib[1,2,3] and James Duncan[1,2,3]

[1]Biomedical Engineering, Yale University [2]Electrical Engineering, Yale University [3]Radiology & Biomedical Imaging, Yale School of Medicine

Introduction

- A displacement vector field (DVF) is crucial to infer the underlying spatial-temporal characteristics of anatomical structures.
- Explicit biomechanical constraints imposed on DVF such as incompressibility often consider biomechanical properties only for specific regions of interest, such as the myocardium.
  - Geometric properties in other structures such as the right ventricle (RV) is not guaranteed.
- To encourage physically plausible transformation, pre-trained variational auto-encoders (VAEs) can be used as regularizers to enforce implicit constraints on the DVF.
  - The VAEs are often trained separately on manually generated datasets which require physical simulations.
  - The regularization performance might be limited by VAEs' generalization ability on new datasets.

Contributions

- We propose a biomechanics-informed regularization explicitly as a prior for DVF estimation to preserve geometric properties.
- Our proposed method shows improvement across different cardiac structures due to the more generic assumption.
- We conduct extensive experiments to show its effectiveness and robustness over other competing regularization schemes.

ACDC Dataset [1]

- The dataset contains 100 patients including
  - 20 healthy patients
  - 20 patients with previous myocardial infarction
  - 20 patients with dilated cardiomyopathy
  - 20 patients with an hypertrophic cardiomyopathy
  - 20 patients with abnormal right ventricle
- End-diastolic (ED) and end-systolic (ES) frames are selected from the sequence.
- Segmentation labels consisting of left ventricle (LV), right ventricle (RV), and epicardium (Epi) for ED and ES frames are given.
- 60 patients, 20 patients and 20 patients are used for training, validation and testing, respectively.

Framework

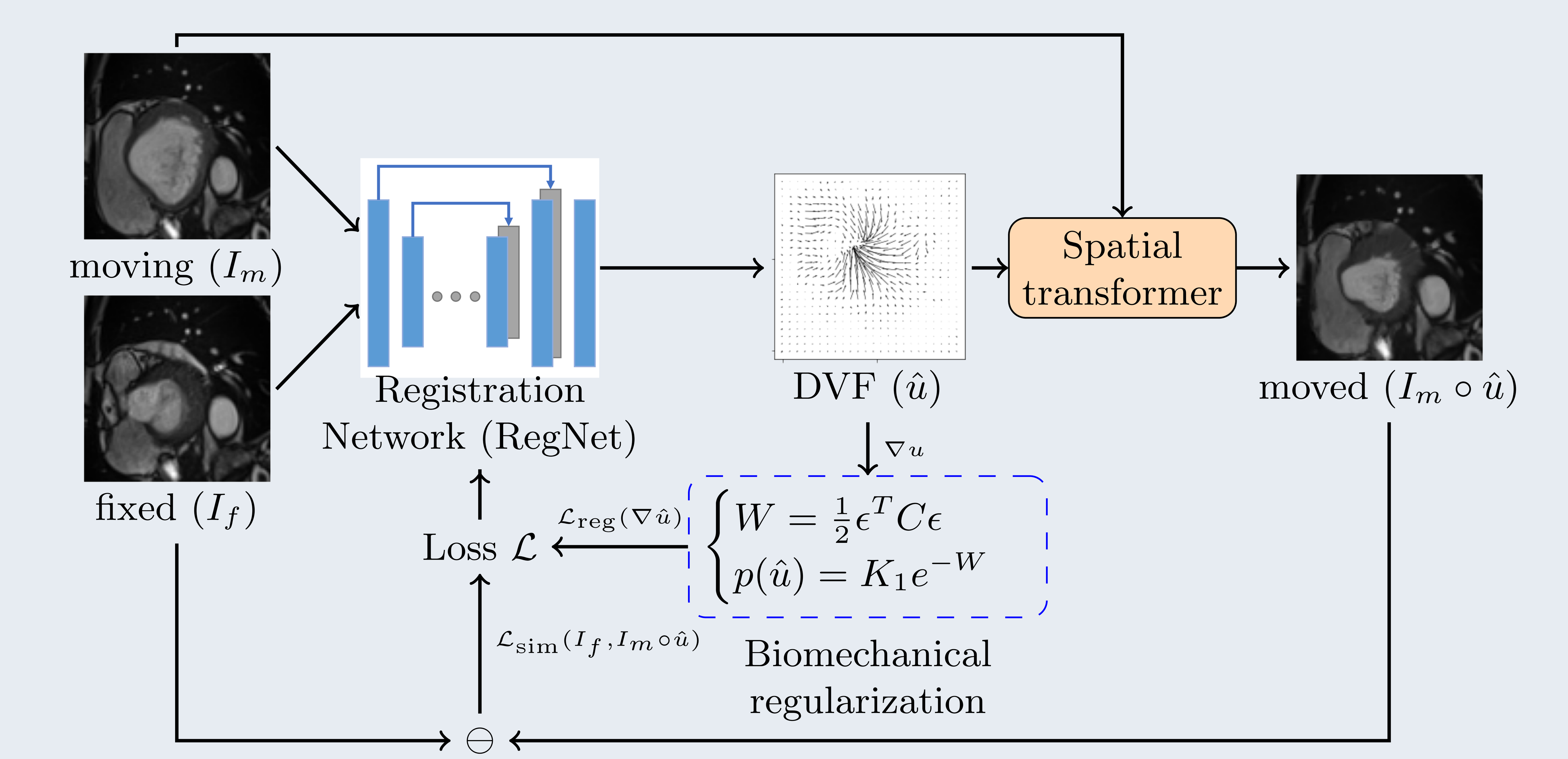

Figure: Illustration of the proposed framework using biomechanics-informed modeling (BIM) for cardiac image registration.

Methods

From the classical definition of the strain tensor $\epsilon \in \mathbb{R}^{3\times H\times W}$ in the infinitesimal linear elasticity model for 2D displacement $\hat{u} = [\hat{u}_1, \hat{u}_2]^T$

$$\epsilon = \left[\frac{\partial \hat{u}_1}{\partial x_1}, \frac{\partial \hat{u}_2}{\partial x_2}, \frac{1}{2}\left(\frac{\partial \hat{u}_1}{\partial x_2} + \frac{\partial \hat{u}_2}{\partial x_1}\right)\right]^T, \tag{1}$$

we define the linear isotropic elastic strain energy density function for each pixel as follows:

$$W_{i,j} = \frac{1}{2}\epsilon_{i,j}^T C\epsilon_{i,j}, \tag{2}$$

where C is the pre-defined stiffness matrix describing material properties of the deforming body. The prior probability density function (pdf) of the DVF can be written in Gibb's form:

$$p(\hat{u}) = k_1 e^{-W}. \tag{3}$$

The optimal DVF $\hat{u}^*$ can be obtained through maximum a posteriori (MAP) optimization:

$$\begin{aligned}\hat{u}^* &= \arg\max_{\hat{u}} \left\{p(\hat{u}|u) = \frac{p(u|\hat{u})p(\hat{u})}{p(u)}\right\} \\ &= \arg\min_{\hat{u}} \left\{-\log p(u|\hat{u}) - \log p(\hat{u})\right\}.\end{aligned} \tag{4}$$

Loss functions

We assume the noise between the ground truth measurement u and the DVF estimate $\hat{u}$ is normally distributed $\mathcal{N}(0, \sigma^2)$

$$p(u|\hat{u}) = \frac{1}{\sqrt{2\pi}\sigma} e^{-\frac{||u-\hat{u}||_2^2}{2\sigma^2}}. \tag{5}$$

We utilize the image dissimilarity between the transformed image $I_m \circ \hat{u}$ and I_f to evaluate the difference of $\hat{u}$ with the ground truth motion field

$$\mathcal{L}(I_m, I_f; \hat{u}) = \underbrace{\frac{1}{N}\sum_{i=1}^{N} ||I_f^i - I_m^i \circ \hat{u}^i||_2^2}_{\mathcal{L}_{sim}} + \lambda \underbrace{\frac{1}{N}\sum_{i=1}^{N} ||\epsilon^T C\epsilon||_2}_{\mathcal{L}_{reg}}, \tag{6}$$

where N is the number of samples. When segmentation masks are available, we can further improve the approximated difference of $\hat{u}$ with ground truth by adding an auxiliary segmentation loss

$$\begin{aligned}\mathcal{L}(I_m, I_f, s_m, s_f; \hat{u}) &= \mathcal{L}(I_m, I_f; \hat{u}) \\ &+ \gamma \underbrace{\frac{1}{N}\sum_{i=1}^{N}\sum_{j=1}^{K}\left(1 - \mathrm{Dice}\left(s_m^{ij} \circ \hat{u}^i, s_f^{ij}\right)\right)}_{\mathcal{L}_{seg}}.\end{aligned} \tag{7}$$

Results

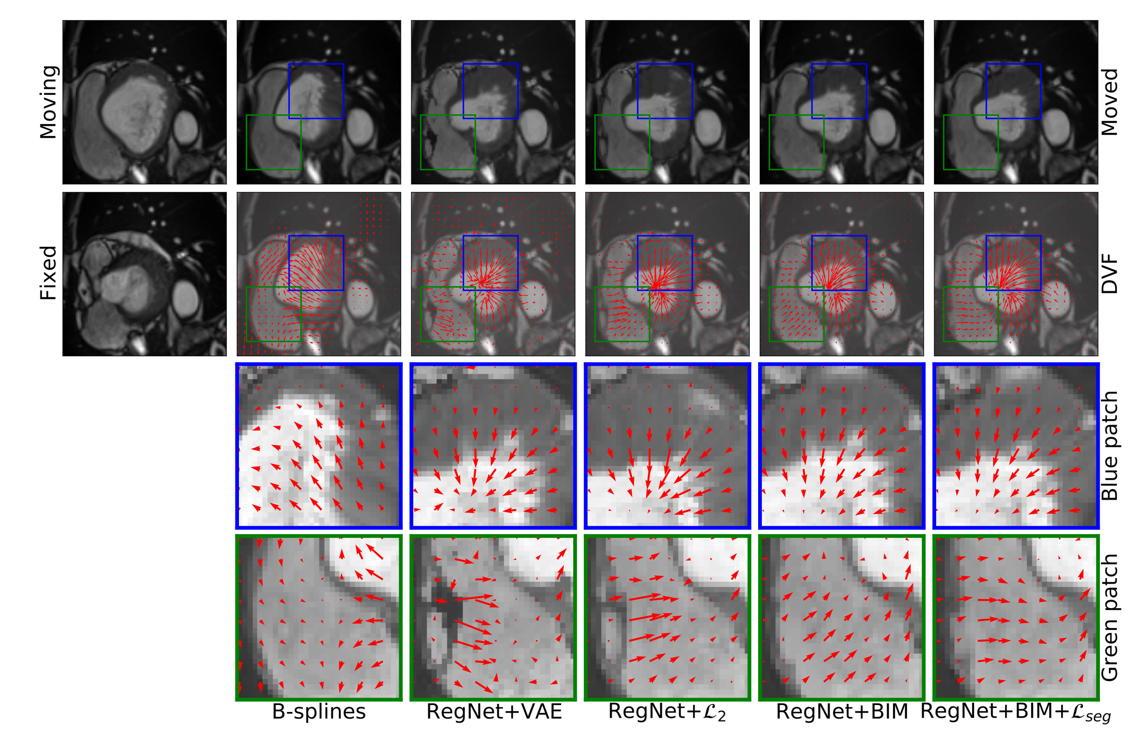

Figure: Visual assessment of DVFs on the ACDC dataset [1].

	Method	Dice[%]↑	Jaccard[%]↑	HD[mm]↓	ASD[mm]↓
	B-splines [3]	89.96	82.62	5.37	0.48
	RegNet+VAE [2]	89.61	81.65	6.46	0.49
LV	RegNet+$\mathcal{L}_2$	89.60	81.68	8.00	0.54
	RegNet+BIM (ours)	90.32	82.70	5.51	0.37
	RegNet+BIM+$\mathcal{L}_{seg}$ (ours)	**92.77**	**86.76**	**4.39**	**0.19**
	B-splines [3]	83.59	74.33	**13.70**	2.43
	RegNet+VAE [2]	84.65	75.58	16.48	2.31
RV	RegNet+$\mathcal{L}_2$	84.80	75.73	14.75	2.25
	RegNet+BIM (ours)	85.07	76.16	14.55	2.22
	RegNet+BIM+$\mathcal{L}_{seg}$ (ours)	**85.93**	**77.54**	14.07	**2.15**
	B-splines [3]	92.33	86.12	5.97	0.33
	RegNet+VAE [2]	91.45	84.83	7.57	0.48
Epi	RegNet+$\mathcal{L}_2$	89.92	82.22	7.77	0.59
	RegNet+BIM (ours)	91.53	84.75	6.20	0.40
	RegNet+BIM+$\mathcal{L}_{seg}$ (ours)	**92.57**	**86.48**	**5.54**	**0.32**

Table: Quantitative assessment of registration performance on the ACDC dataset [1].

Conclusions

- We propose a novel data-driven approach for cardiac motion tracking with biomechanics-informed modeling regularization.
- Our proposed methods outperform other regularization methods on ACDC dataset [1] in 2D cardiac motion estimation using quantitative assessment and generate more realistic DVF in visual assessment.

References

[1] Bernard, O., et al.: Deep learning techniques for automatic MRI cardiac multi-structures segmentation and diagnosis: Is the problem solved? IEEE Transactions on Medical Imaging **37**(11), 2514–2525 (2018)

[2] Qin, C., et al.: Biomechanics-informed neural networks for myocardial motion tracking in MRI. In: International Conference on Medical Image Computing and Computer-Assisted Intervention. pp. 296–306. Springer (2020)

[3] Rueckert, D., et al.: Nonrigid registration using free-form deformations: application to breast MR images. IEEE Transactions on Medical Imaging **18**(8), 712–721 (1999)